

Peptide-based gel in environmental remediation: removal of toxic organic dyes and hazardous Pb²⁺ and Cd²⁺ ions from wastewater and oil spill recovery

Article

Accepted Version

Mondal, B., Bairagi, D., Nandi, N., Hansda, B., Das, K. S., Edwards-Gayle, C. J. C. ORCID: <https://orcid.org/0000-0001-7757-107X>, Castelletto, V. ORCID: <https://orcid.org/0000-0002-3705-0162>, Hamley, I. W. ORCID: <https://orcid.org/0000-0002-4549-0926> and Banerjee, A. ORCID: <https://orcid.org/0000-0002-1309-921X> (2020) Peptide-based gel in environmental remediation: removal of toxic organic dyes and hazardous Pb²⁺ and Cd²⁺ ions from wastewater and oil spill recovery. *Langmuir*, 36 (43). pp. 12942-12953. ISSN 0743-7463 doi: <https://doi.org/10.1021/acs.langmuir.0c02205> Available at <https://centaur.reading.ac.uk/93783/>

It is advisable to refer to the publisher's version if you intend to cite from the work. See [Guidance on citing](#).

Published version at: <http://dx.doi.org/10.1021/acs.langmuir.0c02205>

To link to this article DOI: <http://dx.doi.org/10.1021/acs.langmuir.0c02205>

Publisher: American Chemical Society

including copyright law. Copyright and IPR is retained by the creators or other copyright holders. Terms and conditions for use of this material are defined in the [End User Agreement](#).

www.reading.ac.uk/centaur

CentAUR

Central Archive at the University of Reading

Reading's research outputs online

A peptide based gel in environmental remediation: removal of toxic organic dyes and hazardous Pb^{2+} and Cd^{2+} ions from waste water and oil spill recovery

Biplab Mondal[†], Dipayan Bairagi[†], Nibedita Nandi[†], Biswanath Hansda[†], Krishna Sundar Das[¶], Charlotte J. C. Edwards-Gayle[‡], Valeria Castelletto[‡], Ian W. Hamley[‡], Arindam Banerjee^{†}*

[†] School of Biological Sciences, Indian Association for the Cultivation of Science, 2A & 2B Raja S. C. Mullick Road, Jadavpur, Kolkata-700032. E-mail: bcab@iacs.res.in

[¶]School of Chemical Sciences, Indian Association for the Cultivation of Science, 2A & 2B Raja S. C. Mullick Road, Jadavpur, Kolkata-700032.

[‡]Department of Chemistry, University of Reading, White knights, Reading RG6, 6AD, United Kingdom

Abstract: A dipeptide-based synthetic amphiphile bearing a myristyl chain has been found to form hydrogels in a pH range 6.9-8.5 and organogels in various organic solvents including petroleum ether, diesel, kerosene, and petrol. These organogels and hydrogels have been thoroughly studied and characterised by different techniques including high resolution transmission electron microscopy (HR-TEM), X-ray diffraction (XRD), Fourier-transform

infrared spectroscopy (FTIR) and rheology. It has been found that the xerogel obtained from the peptide gelator can trap various toxic organic dyes from waste water efficiently. Moreover, the hydrogel has been used to remove toxic heavy metal ions, Pb^{2+} and Cd^{2+} from waste water. Dye adsorption kinetics has been studied and it has been fitted by using Freundlich isotherm equation. Interestingly, the gelator amphiphilic peptide gels fuel oil, kerosene, diesel, petrol in a biphasic mixture of salt water and oil within a few seconds. This indicates that these gels may not only find application in oil spill recovery but also are able to be used to remove toxic organic dyes and hazardous toxic metal ions from waste water. Moreover, the gelator can be recycled several times without significance loss of activity suggesting the sustainability of this new gelator. This holds future promise for the environmental remediation by using peptide based gelators.

Introduction:

Supramolecular gels¹⁻¹⁶ consisting of a variety of small organic molecules have attracted researchers' attention in the last few decades due to their various applications in chemical, material and biological sciences.¹⁷⁻²⁰ Among low molecular weight gelators, peptide amphiphiles belong to a special category, because they provide a distinctive opportunity to design soft materials with controllable structural features and specific secondary structures. The predictable structure-function relationships of the naturally occurring amino acids can thus be utilized to obtain materials with desirable properties.²¹ Under suitable physical condition (solvent polarity, pH, temperature), they can self-assemble *via* non-covalent interactions to form a nanofibrous network structure, that can arrest a large amount of solvent molecules to form gels.²²⁻²⁵ Peptide hydrogels offer a variety of applications in biology and medicine including drug delivery,²⁶⁻³⁰ tissue engineering,³¹ 3D cell culture,^{32, 33} antibacterial agents^{16,34} and wound

healing³⁵⁻³⁷. Apart from the above-mentioned applications, peptide hydrogels have been used for waste water treatment,³⁸⁻⁴² oil spill recovery⁴³⁻⁴⁸ and templates for the synthesis of nanoparticles⁴⁹,⁵⁰ and nanoclusters,⁵¹ and catalysis.^{52, 53}

The toxicity of contaminated water is caused by heavy metals and organic dyes. They are most commonly found in the by-products from the metallurgic industries, textile, printing, and other manufacturing sites which uses the techniques of chemical precipitation, flocculation, bio-treatment and so on.⁵⁴⁻⁵⁷ Highly toxic organic dyes and heavy metal ions such as Pb^{2+} , Cd^{2+} , Hg^{2+} , Cr^{6+} and uranium poses a great threat to the environment and human health, and many organic dyes are also toxic and carcinogenic in nature. Untreated dye effluent from industry pollutes water leading to serious hazards for aquatic life and mankind.⁵⁸⁻⁶³ The presence of toxic dyes in water can be harmful to human beings and other living species even at low concentrations because these are generally non-degradable in nature. Toxic metal pollutants, such as lead and cadmium exist widely in industrial waste water (from battery, electroplate and dye industries) and exposure to high amount of these pollutants can lead to accumulation in the human body and the environment for a long period of time.⁶⁴ Cadmium ions usually get accumulated in various human organs and therefore play a significant role in the food chain.⁶⁵ Lead ions, at very low concentration ($< 0.5\mu\text{g/dL}$)⁶⁶, can damage nerve, immune, renal and cardiovascular systems. Lead deposition in the bones, brain, kidneys and muscles, leads to severe developmental disorders, injuries, diseases and even death.⁶⁷ Therefore, the need for a prompt and efficient approach for the removal of dye and heavy metal ion from waste-water is becoming a hot topic for research. The traditional techniques for waste water management are membrane separation, flocculation, ion exchange, electrochemical treatment etc.⁶⁸ However, there are limitations in terms of cost, efficiency and complexity of these processes. The adsorption technique is the most

suitable in batch and continuous processes of industries. Some absorbents regularly used are carbon based materials, polymers, clay minerals and others.⁶⁹⁻⁷³ There are some materials and methods which are very effective towards oil spill and metal ions adsorption.⁷⁴⁻⁸¹ In this context, it is notable that hydrogels, due to their interstitial void spaces, can absorb dyes and heavy metal ions. Hydrogels can also be very useful materials in many other fields apart from the above-mentioned applications.⁸²⁻⁸⁸ On the other hand, xerogels (dried gels) can be used in various fields, such as energy-storage devices, metacomposites, electromagnetic wave absorbing/shielding devices, and others.⁸⁹⁻⁹² Xerogels having π -surfaces can perform similar water remediation and hence these materials can be used as an attractive candidate for waste water management.⁴⁵

Oil-spills at sea and in river water create a great threat to flora and fauna and, mankind. Though there are different methods of oil spill recovery^{43, 44} gels are particularly successful in mopping up the spilled oil from the surface of water.⁴³⁻⁴⁸

Peptide amphiphile containing a long hydrophobic tail with an alkyl chain and a short peptide sequence with a hydrophilic head group can maintain a suitable balance between the hydrophobicity^{93, 94} and hydrophilicity to form hydrogel under suitable conditions. Interestingly, this type of molecule with both lipophilic and hydrophilic part can also be self-assembled in an organic medium under the suitable condition to form a organogel.⁴³ So, this type of gelator molecule is termed as a 'ambidextrous gelator', as it is capable of forming gels in both aqueous medium and non-aqueous, organic solvents. The ambidextrous nature of such gelator molecules can be utilized for some useful purpose. A prime need for human society is to obtain clean and safe water for everyday use. So, it is of great interest to construct and develop a new gelator molecule that can form a hydrogel which can be utilized for removing toxic organic dyes and

hazardous metal ions from waste water and also can form organogels that find applications in oil spill recovery.

Short peptide based gels from our group and others groups have been used for the removal of toxic organic dyes from waste water and these have also been applied for oil spill recovery.^{38, 44-46, 87} These are the examples of bifunctional peptide based gels in environmental remediation. However, there are no examples of peptide based trifunctional gels in the environmental remediation to the best of our knowledge. This study vividly demonstrate a short peptide based trifunctional hydrogel that has been used in environmental remediation: (a) scavenging of toxic organic dyes from waste water, (b) removal of toxic metal ions including Pd²⁺ and Cd²⁺ from waste water and (c) oil spill recovery. Although, selective absorption of cationic /anionic dyes have never been reported previously for peptide based gelators (to the best of our knowledge), it is noticed that a few non-peptide based small molecular hydrogels can be used for selective adsorption of cationic or anionic dyes. Yu and co-workers reported an imidazole based surfactant gelator which can selectively remove anionic dyes over cationic dyes with very high selectivity.⁹⁵ Bhattacharjee and co-workers reported metallogels, which were found to be shown excellent selectivity of the adsorption of cationic dyes and their separation from anionic dyes.⁹⁶

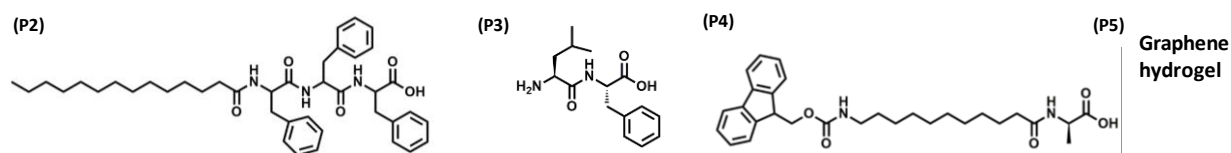
The specialty of this result is that adsorption of cationic dyes by this hydrogel is relatively faster compared to the other peptide based and non-peptide based hydrogels reported from our research group and others. Within only two hours the adsorption of two different cationic dyes (MB and BB) is about 80% (79.2 for MB and 78.4% for BB respectively) and the adsorption of the mixture of dyes either methylene blue and methyl orange (Figure 7e) or methylene blue and bismark brown (Figure 7d) is even faster i.e. 87% approximately for each

case. There is a previous report of the behavior of higher adsorption rate for the anionic dyes from a mixture of dyes, however, these dyes are the mixture of both cationic and anionic dyes unlike this study.^{37, 38, 44, 97} The detailed analysis of the performance of the peptide based hydrogel compared with two previous results is presented in table 1. This indicates clearly the superiority of this peptide based gel compared to our previous results and other's previous results. Moreover, this gel shows selectivity towards the adsorption of cationic dyes over anionic dyes in a mixture of dyes. So, it can be stated that this study exemplifies not only the faster kinetics of adsorption of toxic organic dyes but also exhibits selectivity of cationic dyes over anionic dyes.

Table 1: Comparison of our peptide gelator with different kinds of peptide and non-peptide based gelators in environmental remediation.

Dyes	Peptide Gelator	Non-peptide gelator	Absorption (Within 2hours)	Total Absorption	Total time	References
Methylene blue (MB)	P1		79.2%	98.9% ± 0.2	12h	This report
	P2			98.4%	7 days	37
		P5		98%	72h	81
Congo red (CR)	P1		64%	97.1% ± 0.2	12h	This report
	P3		45%	92%	48h	38
	P4		42%	98%	48h	44
Bismark Brown	P1		78.4%	98.1% ± 0.1	12h	This report
Methylene blue + Methyl Orange	P1		92.7%	98.6% ± 0.3	12h	This report
Methylene blue + Bismark brown	P1		MB:86.98% BB: 86.86%	97.6%± 0.5	12h	This report

Acid black 1 (AB1)	P4		32%	82%	48h	44
Rhodamine B (RB)	P3		38%	78%	48h	38
	P4		32%	71%	48h	44
Direct red 80 (DR-80)	P4		39%	93%	48h	44
Malachite green (MG)	P3		60%	90%	48h	38



In this study, our tripeptide based gelator has been designed in such a way that it is able to attract cationic dyes in presence of anionic dyes selectively. This happens due to the interplay of electrostatic interactions involving two oppositely charged species, as for example anionic xerogel matrix and cationic dyes.

Another specialty of this result is that, this is probably the first example of a peptide based hydrogel that can selectively absorb cationic dyes from a mixture of cationic and anionic dyes. Most probably this is the first report of a small molecule based trifunctional supramolecular gel that has been successfully utilized for environmental remediation. Our previous results show the demonstration of bifunctionality of peptide based gel in environmental remediation. The functionality of peptide based gel needs to be improved to get a clean and safe environment. To achieve this goal this study vividly shows the formation of a trifunctional gel to remove different organic (toxic dyes) and inorganic (Pb^{2+} and Cd^{2+}) pollutants as well as spilled oil from the environment.

This report describes the discovery of a peptide based ambidextrous tri-functional new gelator that has been used to remove toxic organic dyes (cationic and zwitterionic dyes) from waste water and toxic heavy metal ions (lead, cadmium) also from waste water using xerogels and hydrogels respectively. The organogels formed by this gelator, have further been used in oil spill recovery. Another interesting feature is that this gelator is economically viable and reusable several times without significant loss of its activity.

Experimental details:

The peptide amphiphile myristicacid-L-tryptophan-L-phenylalanine-COOH (**P1**) was synthesized using a conventional solution phase DCC/HOBt-mediated coupling method by racemization-free fragment condensation strategy. The C-terminus was protected as a methyl ester. All compounds were purified by column chromatography using silica gel (100-200 mesh size) as stationary phase by using chloroform-ethyl acetate or chloroform-methanol as eluents. Finally, purified compounds were characterized using ^1H NMR, ^{13}C NMR and mass spectrometry. Detailed information about synthesis and characterisation are given in the Supporting Information.

Dye Adsorption Studies:

For each dye adsorption study, 5mg of gelator molecule was taken into a 5mL screw cap vial. Then it was heated on a hot plate by adding 1mL of phosphate buffer solution (PBS) having pH 7.46. After dissolving all the gelator molecules into the PBS, the vial was cooled for few minute (10 min) to room temperature to make the hydrogel **P1**. Then, the gel was frozen in liquid nitrogen and lyophilized. After that a pellet of dried gel (xerogel) had been made by using pelletizer instrument. The pellet was taken into a 5mL screw cap vial and 1mL of aqueous dye

solutions were carefully added to the vial. During dye adsorption study the concentrations of methylene blue, bismark brown and congo red were 3.0mg/L, 2.0mg/L and 2.0mg/L respectively. After that at a definite time interval 15 min, 30 min, 60 min, 120 min, 180 min, 360 min and 720 min dye adsorption data were collected by using UV-vis spectroscopy.

Metal Ion Removal Studies:

Atomic absorption spectroscopy (AAS) was performed to determine the efficiency of the hydrogel for Cd^{2+} ion absorption. An amount of 100 μL 50mM cadmium chloride monohydrate ($\text{CdCl}_2 \cdot \text{H}_2\text{O}$) solution was added to 5mL of ultrapure water to prepare a stock solution. From this stock solution 1mL $\text{CdCl}_2 \cdot \text{H}_2\text{O}$ was taken and added to 1mL of hydrogel in the phosphate buffer (pH 7.5). The concentration of the Cd^{2+} ions in the initial solution was determined through AAS using a standard calibration curve. After 8h, a 30 μL aliquot was taken from the solution which is in contact with gel and this solution was diluted to 10mL by mixing with mili-Q water (pH 6.7) in order to examine the amount of Cd^{2+} ions retained after the absorption by the hydrogel. An aliquot of 10 μL 50 mM solution of lead nitrate $\text{Pb}(\text{NO}_3)_2$ was added to a 1 mL of mili-Q water. Then this diluted lead nitrate solution was added on the top of 1mL of hydrogel. After 8h, a 10 μL aliquot was taken out and it was diluted with 10mL of mili-Q water. The Pb^{2+} ions adsorption capacity was measured by inductively coupled plasma atomic emission spectroscopy (ICP-AES) as it is a good technique for the determination of concentration of metal ions in different solutions.

Oil Spill Recovery:

Gelator amphiphile (**P1**) was first dissolved in a minimum volume of ethyl acetate (5 % v/v) and was injected (100 μ L of the stock solution was used for injection in each set) into 2 ml of a 1: 1 salt water (water containing NaCl, Na₂SO₄)–oil mixture.

Recovery and Reusability of the Gelator:

The recovery of the gelator, from the hydrogel and xerogel mixed heavy metal ions and dye molecules, was simply done by extracting it in ethyl acetate, using a separating funnel. For the xerogels adsorbed dye molecules, simple extraction with ethyl acetate was sufficient, as the dyes preferred to remain in aqueous medium; whereas in the case of hydrogels containing adsorbed metal ions, 1mL of hydrogel was treated with 20 μ L of 1(N) hydrochloric acid before extraction of the gelator peptide amphiphile in ethyl acetate.

Recovery of Oil:

The gelled oil part was taken out from the vial with the help of a spatula. Then the gelled oil was taken into a round bottom flask and distilled by using a low vacuum rotary evaporator to get the oil part in to the collector. The gelator compound remained in the round bottom flask and it was further used for the recovery of another set of oil spill.

Results and Discussion:

Gelation studies: A peptide amphiphile (Figure 1) consisting of two aromatic amino acid residues (L-tryptophan and L-phenylalanine), a terminally placed polar head group (-COOH) and a long fatty acyl chain as a hydrophobic tail was designed. Specifically, aromatic amino acid

residues were selected to promote π - π interactions, amide functionalities for hydrogen bonding interactions, hydrophobic long chain for van der Waals interactions and the terminally located carboxylic acid (-COOH) head group was chosen to increase the polarity of the peptide molecule. Moreover, the amphiphile was designed in such a way that it can easily form a hydrogel as well as organogels by using polar aqueous and nonpolar organic media respectively. To investigate the gelation behavior, 5 mg of the gelator was placed in a 5 mL screw capped glass vial with the addition of 1 mL of different types of solvent including water (phosphate buffer solution of pH 7.46). The glass vial was heated on a hot plate until the solute is dissolved into that particular solvent. After that, the glass vial was kept at room temperature (27°C) for a few minutes (depending upon the solvent) to form a stable gel (Figure 1). The compound was insoluble in *n*-hexane but soluble in ethyl acetate, an antisolvent-induced gelation study was performed to investigate the gelation behavior of peptide amphiphile. Only 5% ethyl acetate (v/v) was used with respect to *n*-hexane to have rapid (approx. 30 s) gelation (Table S1).

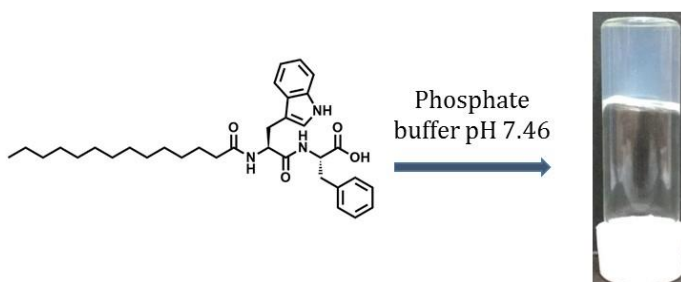


Figure 1. Structure of the peptide amphiphile that forms hydrogel at phosphate buffer solution of pH 7.46.

Morphological studies:

High resolution transmission electron microscopy (HR-TEM) imaging was performed in order to explore the morphological features of the peptide-based hydrogel. It is observed that the gelator

molecule assembles to form a cross-linked nanofiber network structure in the gel state. These fibers are several micrometer (μm) in length, with width varying from 31.7 nm to 64.0 nm (Figure 2a). Whereas the organogel formed by using 5% ethyl acetate in n-hexane solution also shows a cross linked network structure in gel state. The width of the organogel was found 38.16 nm to 54.21 nm(Figure 2b). To understand the morphological change in hydrogel, HR-TEM images were taken at different pHs of 6.9, 7.46 and 8.5 respectively. Interestingly, at all these three pHs, only nanofibrous microstructure was observed (Figure S4).

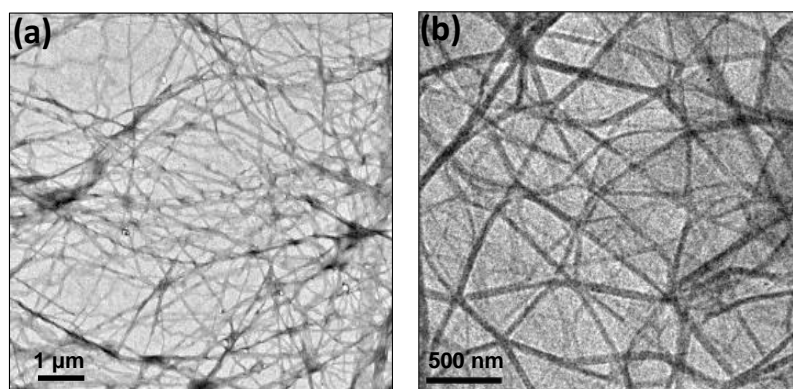


Figure 2. High Resolution Transmission Electron Microscopic (HR-TEM) images of (a) hydrogel at pH 7.46 and (b) organogel in n-hexane.

Fourier Transform Infrared (FT-IR) Analysis: FTIR experiments were conducted to provide structural insight on the packing of gelator molecule **P1** in dried gels (organogel or hydrogel) in their respective solvents. Figure S5 indicates that the dried gel obtained from the organogel and also from hydrogel show sharp signals at around 3320 cm^{-1} , 1646 cm^{-1} and 1547 cm^{-1} respectively. The strong signal at around 1646 cm^{-1} is due to the stretching of the amide C=O group of the aggregated gelator molecules. Two other peaks at 3320 cm^{-1} and 1547 cm^{-1} correspond to hydrogen-bonded N-H stretching and N-H bending frequencies respectively. The peak at around 3415 cm^{-1} for hydrogel indicates the non-hydrogen bonded stretching frequency

of the N–H bond which is found to be very weak in intensity for the organogel. This observation indicates that unlike the hydrogel, almost all the N-Hs form hydrogen bonds inside the organogel (Figure S5).

Rheological studies: Rheological experiments were carried out at a constant gelator concentration 0.5 (w/v) (8.91mM) to examine the viscoelastic characteristics of the gels obtained from the self-assembling peptide **P1** in aqueous medium (pH 7.46) as well as in organic solvent, n-hexane. All frequency sweep experiments were performed under a constant strain of 0.05% and it is observed that storage modulus (G') is almost independent of angular frequency within the tested frequency range and storage modulus (G') is always greater than loss modulus (G''), which indicates the characteristic feature of a gel phase material (Figure 3). At an angular frequency 10.5 rad/s, the storage modulus of the hydrogel is 920 Pa, whereas at the same angular frequency loss modulus is 305 Pa, i.e. the high storage modulus (G') value signifies the gel state of our materials (Figure 3a). Interestingly, the stiffness of the organogel obtained from the same gelator is much more than the hydrogel. Making comparison at a fixed frequency 10.5 rad/s, G' increases from 920 Pa for the hydrogel to 13494 Pa for the organogel in n-hexane (Figure 3b), a near 15-fold increase. These results show that the mechanical strength of the gel is enhanced significantly by the change of the solvent medium from water to an organic solvent (n-hexane). The change in solvent triggers a very significant increase of the gel storage modulus. The amplitude sweep experiments were done to determine the limits of linear viscoelastic region (LVE) of both gels. The hydrogel shows tolerance limit between 0.01% and 1.18% of shear strain (Figure S6a). Moreover, it was found that it showed a cross-over of storage modulus (G') and loss modulus (G'') when 6% shear strain was applied to the sample. Whereas, the tolerance limit of the organogel sample lies between 0.01% to 0.56% (Figure S6b) and the cross-over

between G' and G'' took place, when 20% of shear strain was exerted on the sample. To confirm the thixotropic behavior of the hydrogel, time dependent step strain experiment was carried out with a time step 125s (Figure S6c, d). Initially strain was increased from 0.05% to 30% at which the rupture of gel phase takes place, i.e. gel to sol conversion occurs. After that, when strain was reduced to 0.05%, reformation of gels were observed and this process was continued for 5 times to show the reproducibility of both gels(Figure S6c, d). It was observed from the FT-IR studies that both non-hydrogen and hydrogen bonded N– H stretching frequencies are present in the case of hydrogel, while in case of organogel almost all N– Hs of the gelator molecule are hydrogen bonded. The presence of extra H-bonding in the organogel can be attributed to greater stiffness of this gel which is reflected into this rheology data.

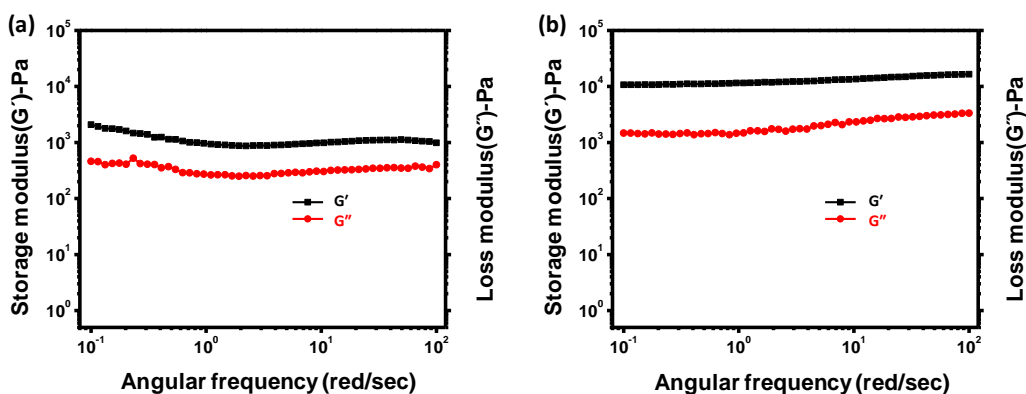


Figure 3. Frequency sweep analysis of (a) hydrogel and (b) organogel in *n*-hexane at a constant strain of 0.05%.

X-Ray Diffraction (XRD) analysis:

The wide angle X-ray diffraction (XRD) data from xerogels obtained from the hydrogel, a peak at $2\theta = 18.45^\circ$ corresponds to a d -spacing value 4.68 \AA indicating the inter-planar distance between two β -strand. Peaks at $2\theta = 22.80^\circ$ and $2\theta = 23.58^\circ$ with d -spacing values 3.79 \AA and

3.67 Å are due to π - π stacking, consistent with the presence of aromatic groups into the gelator molecule (Figure 4b).³⁷ In the small-angle XRD profile, the peak at $2\theta = 2.61^\circ$ ($d=33.57$ Å) arises from the gelator molecule in the gel state (Figure 4a). In the case of xerogel obtained from the organogel (in *n*-hexane), the peaks (Figure 4d) at $2\theta = 8.92^\circ$ ($d=9.64$ Å) and $2\theta = 18.61^\circ$ ($d=4.64$ Å) are due respectively to the inter-sheet distance and the inter-planar distance between two β -strands of the aggregated peptide amphiphile **P1**. The peak at $2\theta = 21.99^\circ$ with d -spacing 3.90 Å is due to aromatic stacking interactions between two gelator molecules (Figure 4d). In the small angle region, a peak at $2\theta = 3.14^\circ$ with d -spacing 28.09 Å is also due to the intermolecular spacing in the gel (Figure 4c).

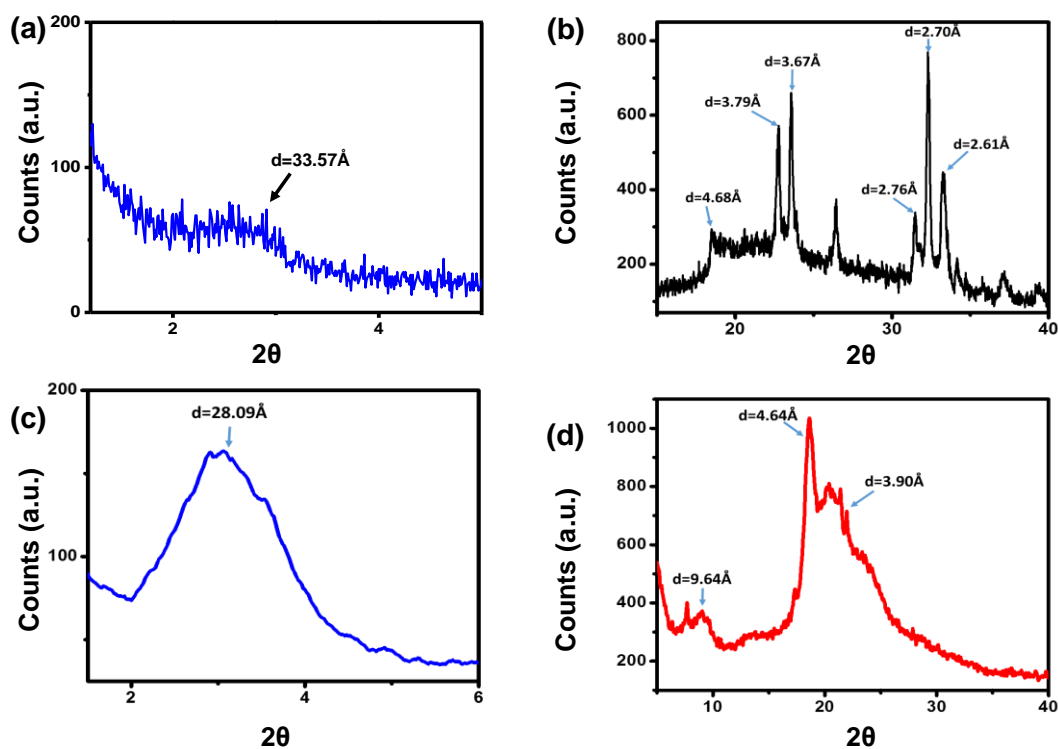


Figure 4.(a) Small-angle and (b) wide-angle X-ray diffraction pattern of xerogel obtained from hydrogel, (c) small-angle and (d) wide-angle X-ray diffraction pattern of xerogel obtained from organogel in *n*-hexane.

Small angle X-ray scattering (SAXS) analysis:

To complement the small-angle XRD data obtained from xerogels, in situ SAXS measurements were performed on hydrogels. The intensity profile shown in Figure 5 for the **P1** hydrogel contains a broad Bragg peak with a d -spacing of 40\AA , which is longer than the length of a single molecule and also does not match with double the molecular length. Thus, this distance indicates end-to-end packing of peptide gelator molecules arranged in an interdigitated manner as shown in Figure 6. A tentative packing arrangement of the gelator molecules in the gel state is proposed based on Fourier-transform infrared spectroscopy (FTIR), small and wide angle powder X-ray diffraction (PXRD) and small angle X-ray scattering (SAXS) data (Figure 6).

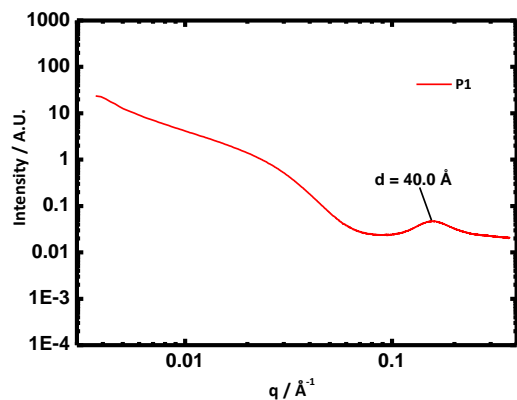


Figure 5. Small angle X-ray scattering (SAXS) data of hydrogel (**P1**).

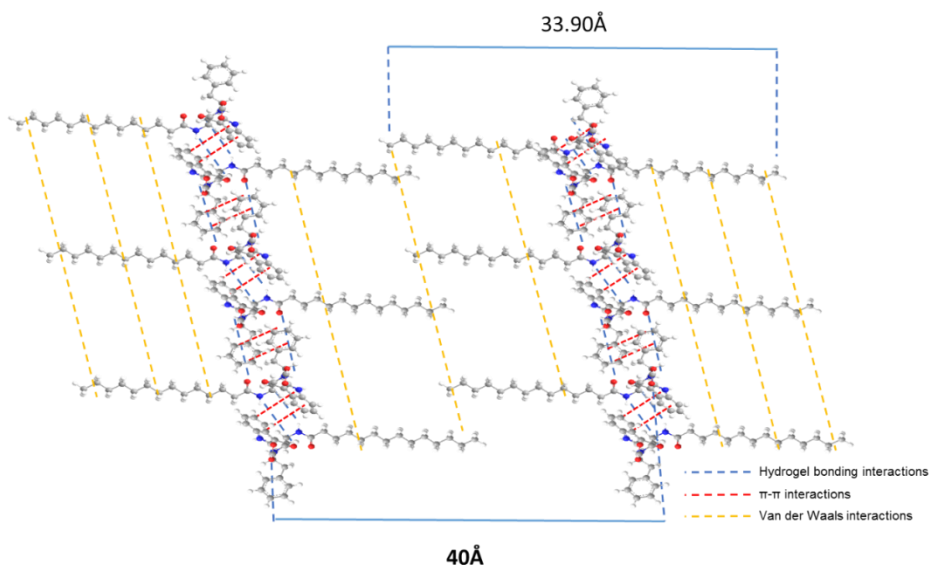


Figure 6. A tentative model of inter-molecular arrangements in the hydrogel derived from small angle X-ray scattering (SAXS), X-ray diffraction and FTIR data.

Dye Adsorption Studies:

Removal of toxic organic dyes from waste-water is a long-standing problem, as these dyes not only contaminate river and other water resources, but also endanger aquatic biota. So, it is important to explore new efficient methods for removal of these environmentally hazardous substances from waste-water.

Porous gels are potentially useful materials for removing toxic organic dyes from contaminated water. The hydrogel obtained from the peptide gelator **P1** has been used for removing cationic and neutral dyes effectively. Dyes like methylene blue (MB), bismarck brown (BB) and congo red (CR) are regularly used in textile industry. The hydrogel of **P1** is prepared in phosphate buffer solution of pH 7.46 and it was dried to get the xerogel. Adsorption studies were done by using the dried gel to nullify the effects of diffusion of dye from the solution to trapped water in the hydrogel network. Methylene blue and bismarck brown being cationic dyes, were adsorbed in the anionic xerogel network very fast. 90.3% of MB and 86.4% of BB of the dye solution were adsorbed in only three hours. It is found that the xerogel adsorb each of these dyes MB and BB separately more than 85% within only three hours and this result is better than the previous report^{38, 44}. Whereas the neutral dye used in the experiment, congo red shows an adsorption of 65% in three hours. Almost complete adsorption of MB (98.9%) and BB (98.1%) has been observed within 24 hours. On the other hand, 97.1% adsorption of congo red has been observed within 48h. Adsorption kinetics was studied with a mixture of dyes MB and BB. The dye

adsorption kinetics of each dye is similar as it is evident from the experimental studies (Figure 7).

Our result shows the reusability of dried gel for several times (three times) without any significance loss of efficiency (Figure S7a). Moreover, this peptide based dried gel (xerogel) has been used for adsorption of more than one dyes (methylene blue and bismark brown) from a mixture of dyes indicating its probable use in real life system for the waste water treatment, where more than one dyes are found in the contaminated water. It is found that the cationic dyes (methylene blue and basic brown) are strongly adsorbed compare to neutral dye (congo red), as it is evident from the Table 1 that per gm of gelator molecules is able to adsorb 629 mg of methylene blue and 406 mg of bismark brown, whereas same amount of gelator molecule is able to absorb 165 mg of congo red. Dye adsorption kinetics was done by taking MB and BB separately and also the kinetics was done by taking their mixture (Figure 7a, b and d). To understand the mechanism of the adsorption of dyes on the xerogel matrix, dye solutions of different concentrations were charged on the absorbent xerogel and equilibrate for 12 hours. Both congo red and methylene blue showed good fitting in the Freundlich isotherm model which signifies the adsorption happened in multilayer mechanism (Figure 9a and 9b). Several anionic dyes have been used for adsorption by using self-assembled peptide based gels, none of these dyes were adsorbed by the xerogel indicating its selectiveness to adsorbing dyes towards basic (cationic) and neutral (non-ionic) dyes (Figure 7e). This can happen due to the fact that our peptide gelator is anionic at pH 7.46 at which it forms gel and all these adsorption studies were performed at this pH. Due to the electrostatic interaction between the gelator molecules and cationic dyes, the cationic dyes are adsorbed more and the non-ionic dyes are adsorbed to a lesser extent compared to the cationic dyes. However, the charge-charge repulsion between the

gelator molecule and anionic dyes prevents the peptide gel (in this study) to adsorb any kind of anionic dyes. Reusability experiments were carried out in order depict to its large scale utility. The dye absorbed xerogels were recovered by using ethyl acetate-water interface, where the dye remained in water and the gelator **P1** was extracted from ethyl acetate. For the next cycle, hydrogels were reformed using those gelator **P1** molecules and it was freeze-dried before next set of absorption experiment. Table S3 clearly demonstrates the detailed reusability study including the percentage of loss of compound as well as the loss of activity for the removal of toxic dyes, metal ions and oil spill recovery in waste water treatment. From the Table, it can be clearly noted that **P1** can be recovered three times for reusing purpose without significant loss of its activity (Figure S7). This is because, after the third time, the amount of recovered gelator is not enough to form gel. However, the recycling can be done for another two times for the metal ion adsorption (Figure S7). After, the metal ion adsorption, no physical change is observed in the hydrogel. The recovery of gelators is done according to the previously mentioned procedure in the dye absorption section (Figure S7). In the case of reusability study for the oil spill recovery, oils were recovered from the organogel by vacuum distillation and gelator molecules were separated from the gel phase. During this study no physical change was observed in the organogel. The recovered gelator molecules were used for re-gelling of the spilled oil. Finally, it was observed that the gelator amphiphile can be used three times (Figure S9) for the recovery of different sets of oil spill without any significant loss of the activity.

As we know, Freundlich adsorption isotherm model is expressed as-

$$\log q_e = \log K_f + \frac{1}{n} \log C_e \quad (a)$$

where, q_e is the equilibrium adsorption capacity of dye adsorbed on xerogel surface, C_e is the

equilibrium concentration of the adsorbate(mg/L), K_f is the Freundlich constant and n is the heterogeneity factor of Freundlich adsorption isotherm. From methylene blue and congo red dyes data it is observed that the slope($1/n$) of Freundlich adsorption isotherm fitted plot Figure 9a and Figure 9b are 4.42 and 1.23 respectively. This data clearly matches with the rate of dye adsorption data showing in to the Figure 7a and Figure 7c.

Adsorption kinetics experiments have been done systematically. Kinetic study for the adsorption of methylene blue dye was done at different time intervals at a constant room temperature (22°C)and these data were fitted against both pseudo-first order and pseudo-second order kinetics using the following equations⁹⁸(Figure 10).

$$\log(q_e - q_t) = \log q_e - \frac{k_1 t}{2.303} \quad (b)$$

$$\frac{t}{q_t} = \frac{1}{k_2 q_e^2} + \frac{t}{q_e} \quad (c)$$

Where, q_e and q_t are the amount of adsorbed dye (mg of dye per gof the gelator) at equilibrium time and at the time t (min) respectively, k_1 is the pseudo-first order rate constant (min^{-1}) and $k_2(\text{min}^{-1})$ is the pseudo-second-order rate constant. The coefficient of determination (R^2) for the pseudo-second-order kinetic model was much higher ($R^2 = 0.99986$) than that of the pseudo-first-order kinetic model ($R^2 = 0.72453$), which indicates the adsorption of methylene blue dye follows pseudo-second-order kinetics. The dye adsorption data for cationic dye methylene blue fits well with the pseudo-second order reaction kinetics than the pseudo first order kinetics.

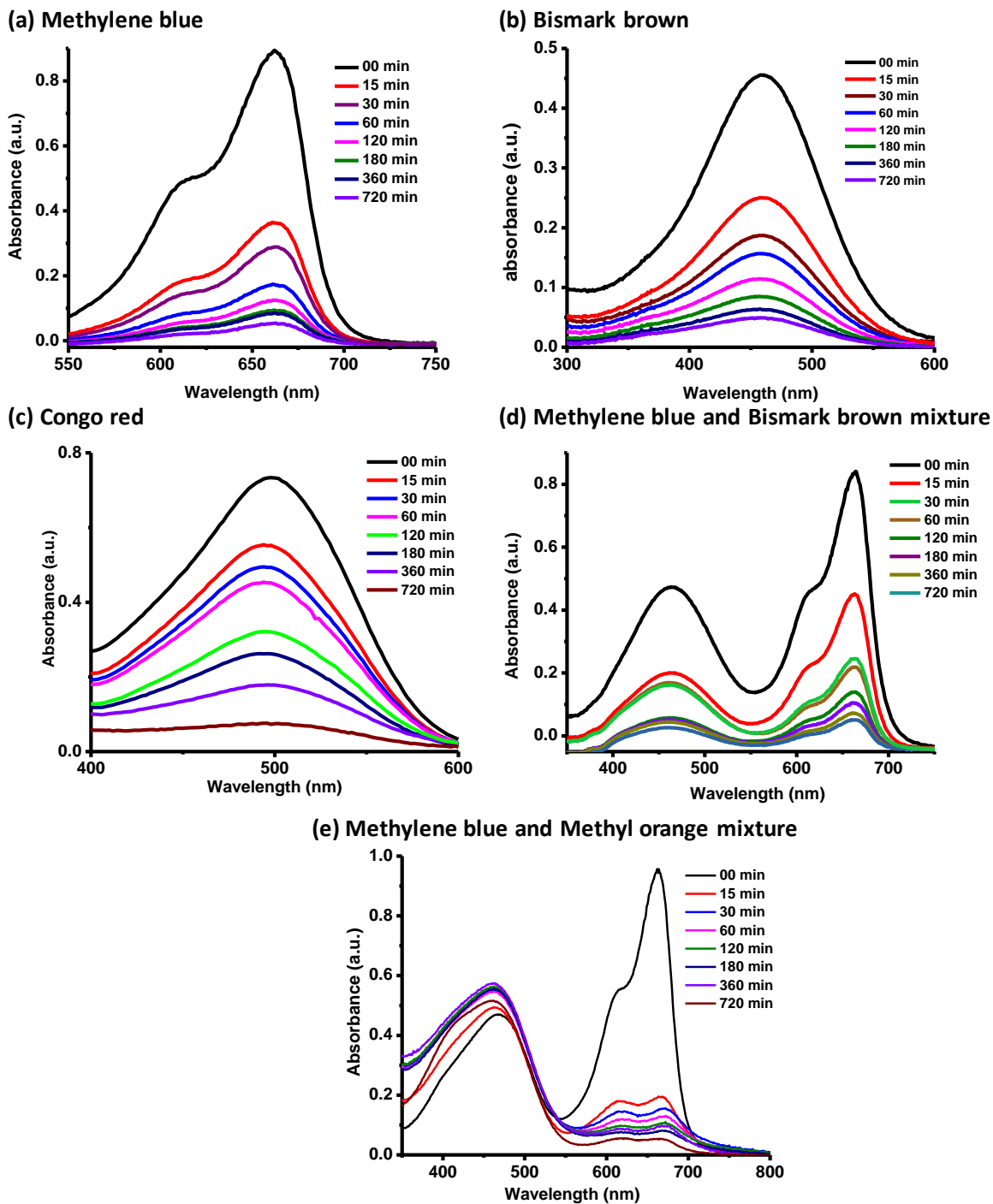


Figure 7. UV-vis spectroscopic study of dye adsorption of (a) methylene blue, (b) bismark brown, (c) congo red, (d) mixture of methylene blue and bismark brown and (e) mixture of methylene blue and methyl orange at 22°C indicating the specific adsorption of methylene blue (cataionic dye) from a mixture of both cataionic and anaionic dyes.

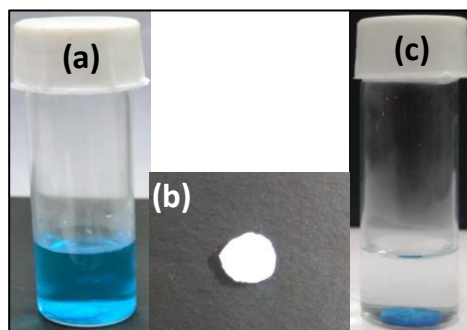


Figure 8. Photography (a) corresponds to the xerogel in methylene blue solution, (b) pellet of dried gelator molecule **P1** made by pelletizer and (c) methylene blue adsorbed xerogel and fresh water after 24h at 22°C.

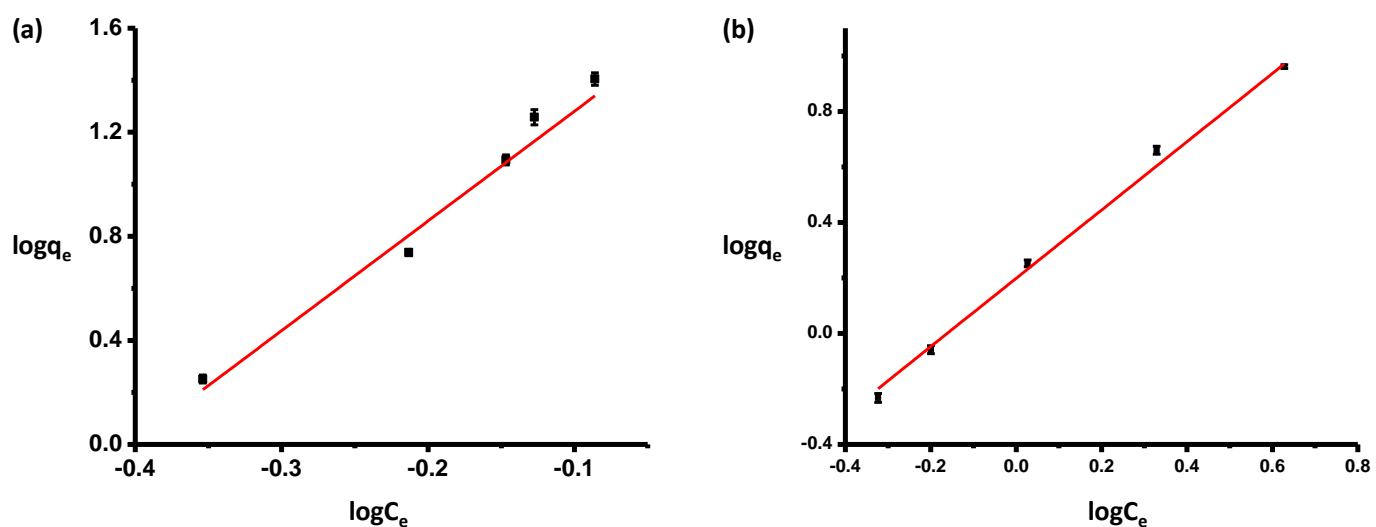


Figure 9. (a) Freundlich adsorption isotherm fitted dye adsorption data of methylene blue and (b) Freundlich adsorption isotherm fitted dye adsorption data of congo red with error bars at an average temperature 25°C.

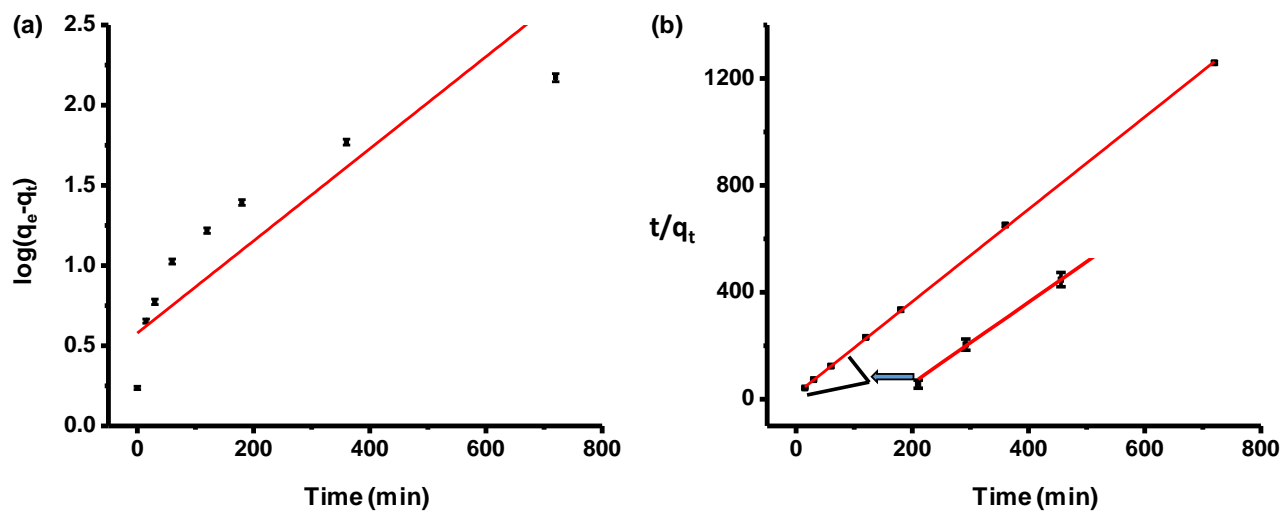


Figure 10. (a) Fit of kinetic data to pseudo-first-order model and (b) Fit of kinetic data to the pseudo-second-order model for methylene blue dye with error bars indicating the fact that it fits well with pseudo-second-order kinetics (First three data points are enlarged to show the error bars clearly).

Table 2: Dye adsorption by xerogel, obtained from UV-vis measurements at 22°C.

Dye	Nature	% removal	Amount of dye absorbed by per gm of gelator (mg)
Methylene blue	Cationic	98.9% ± 0.2	629.3 ± 4.6
Bismark brown	Cationic	98.1% ± 0.1	406.0 ± 2.1
Congo red	Neutral	97.1% ± 0.2	165.7 ± 7.7

Metal ions removal studies:

Toxic heavy metal pollutants, such as lead and cadmium are found in industrial waste-water and are hazardous towards the environment and have detrimental effects on human health causing cancer, bone damage, kidney damages and other fatal diseases.⁵¹ Thus, it is important to remove both Pb^{2+} and Cd^{2+} ions from contaminated water.

The initial concentrations of Cd^{2+} and Pb^{2+} ions were 2.54 ppm and 2.13 ppm for the freshly made metal ion solution respectively. After adsorption it was observed that the concentrations of Cd^{2+} metal ions were 0.054 ppm for hydrogel. As a result, it was found that the hydrogel removes 97.88% of Cd^{2+} ions (Table S2). Moreover, this gel is able to remove nearly all the toxic heavy metal ions from waste water. The maximum loading capacities of Cd^{2+} ions for the hydrogel was found to be 21.75 mg by per 1mL of gel (5mg gelator in 1mL buffer solution).

However, the concentration of Pb^{2+} was 0.024 ppm for the hydrogel after the adsorption of Pb^{2+} ions, corresponding to 98.8% adsorption for the hydrogel (Table S2). The adsorption of toxic Pb^{2+} ions using this hydrogel is comparable to that reported previously for a tripeptide-based gelator.³⁸ After the metal ion adsorption, no physical change is observed in the hydrogel. The recovery of gelators is done accordingly previously mentioned procedure in the dye adsorption section. While for metal ion adsorption, the recycling can be done twice. (Figure S7)

Oil spill recovery:

Peptide amphiphiles are potentially valuable in producing gels to recover oil spills from the ocean. In this regard, biphasic mixtures of salt water and oil were prepared with different types of oils including *n*-hexane, petroleum ether, diesel, petrol and kerosene. We investigated gelation using **P1** in a salt water/oil mixture. As shown in Figure 11, gelation of the oil part was observed within 30 s after addition of the gelator solution. To the best of our knowledge, this is the first

example of a tryptophan-based ambidextrous gelator which is able to selectively gel fuel oils from a salt water–oil mixture. Previous example of biphasic gelation from oil water mixtures includes the example of an amino acid containing amphiphile with a long fatty acid chain showing phase selective gelation for oil spill recovery and other examples include urea-based gelators and other low molecular weight gel-formers which gel fuel oils in oil-water biphasic mixture.⁴³⁻⁴⁸ There are several examples on TiO₂ based mechanically robust hybrid coatings,⁷⁸ nanocellulose based aerogels,⁹⁹ magnetic aerogels¹⁰⁰ and nano-dimensional hydrophobic materials^{101, 102} for effective oil absorptions from biphasic oil-water mixtures, reported so far in literature. However, these methods have shortcomings, sometimes due to inherent toxicity, costly regeneration processing and sometimes due to difficulty in the recovery of oil from the separated substances. Gels are emerging materials for phase-selective oil spill recovery and these are very important materials to study as they are cost-effective systems with important application in waste remediation. The current gel material has high effectiveness with respect to oil spill. Our system can absorb or gelify fuel oil, kerosene, diesel, petrol in a biphasic mixture of salt water and oil within 30 seconds and the absorption capacity of this gelator to gelify different fuel oils from waste water varies from 194gm to 205gm of fuel oils per gm of the gelator.

Therefore, it can be stated that regarding oil-spill recovery from waste water, our peptide based ambidextrous gel material is comparable with previously mentioned studies. It is neither superior nor inferior to the previously mentioned gel based materials for oil-spill recovery. However, the efficiency of this gel to selectively gelify fuel oils from a salt water–oil mixture is good and this gel is recyclable for further use. Moreover, this peptide based gelator shows three distinct activities for environmental remediation: oil-spill recovery, toxic organic dyes removal

and heavy metal-ions removal from contaminated water. The main goal of our work is to project a tri-functional gelator, which can be used in multiple ways for the remediation of water pollution. From oil spill recovery and reusability study, oils have been recovered from organogel by vacuum distillation and gelator molecules were separated from the gel phase. During this study no physical change was observed in the organogel. The recovered gelator molecules were used for regelling of spilled oil. Finally, it was observed that the gelator amphiphile can be used three times (Figure S9, Table S3) for the recovery of different set of oil spill (Figure S8).

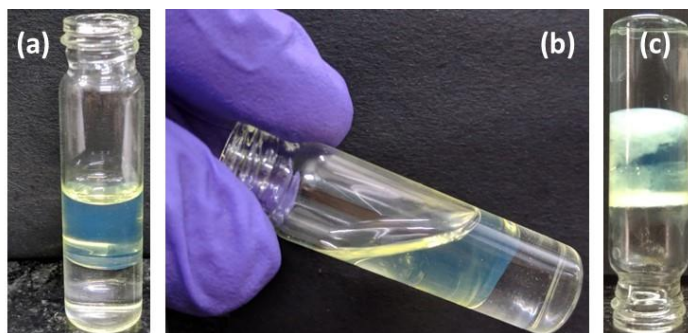


Figure 11. Images (a) biphasic oil-salt water, (b) liquid state of biphasic oil-salt water mixture, (c) self-supporting organogel formed after the addition of peptide amphiphile dissolved in 5% (v/v) ethyl acetate in the oil phase (diesel).

Conclusions:

A new peptide-based gelator is developed and is shown to form hydrogel within the pH range 6.9-8.5. It is able to effectively gel many organic solvents including petroleum ether, diesel, kerosene, petrol etc. from a biphasic mixture. The xerogels obtained from hydrogels have been successfully utilized to remove toxic organic dyes and hydrogels for hazardous heavy metal ions including lead and cadmium from waste water. Moreover, the peptide selectively gels fuel oil (forming an organogel phase) in a mixture with salt water-oil mixture including its probable use in oil spill recovery. The reusability of this peptide based gelator molecule without significant

loss of activity is another notable feature of the peptide amphiphile. Thus, this peptide gelator shows three distinct activities for environmental remediation. Our results show, there is great future promise for self-assembling peptide amphiphile as novel smart soft materials for the removal of various pollutants from the environment.

Notes:

The authors declare no competing financial interest.

Acknowledgements:

B. M, D.B and B.H want to acknowledge UGC, K.S.D thanks DST-INSPIRE and N. N thanks IACS, Kolkata for fellowships. I.W.H thanks EPSRC for Platform grant EP/L020599/1 which supported V.C. and Diamond Light Source and the University of Reading for a studentship for C.J.C.E.-G. and the award of beam time (ref. sm17118-1).

References:

- (1) Cross, E. R.; Sproules, S.; Schweins, R.; Draper, E. R.; Adams, D. J. Controlled Tuning of the Properties in Optoelectronic Self-Sorted Gels. *J. Am. Chem. Soc.* **2018**, *140*, 8667–8670.
- (2) Kaufmann, L.; Kennedy, S. R.; Jones, C. D.; Steed, J. W. Cavity-Containing Supramolecular Gels as a Crystallization Tool for Hydrophobic Pharmaceuticals. *Chem. Commun.* **2016**, *52*, 10113–10116.
- (3) Du, X.; Zhou, J.; Shi, J.; Xu, B. Supramolecular Hydrogelators and Hydrogels: From Soft Matter to Molecular Biomaterials. *Chem. Rev.* **2015**, *115*, 13165–13307.

- (4) Das, S.; Okamura, N.; Yagi, S.; Ajayaghosh, A. Supramolecular Gel Phase Controlled [4 + 2] Diels-Alder Photocycloaddition for Electroplex Mediated White Electroluminescence. *J. Am. Chem. Soc.* **2019**, *141*, 5635–5639.
- (5) Liyanage, W.; Nilsson, B. L. Substituent Effects on the Self-Assembly/Coassembly and Hydrogelation of Phenylalanine Derivatives. *Langmuir* **2016**, *32*, 787–799.
- (6) Marti-Centelles, R.; Escuder, B. Morphology Diversity of L-Phenylalanine-Based Short Peptide Supramolecular Aggregates and Hydrogels. *ChemNanoMat* **2018**, *4*, 796–800.
- (7) Draper, E. R.; Adams, D. J. Controlling the Assembly and Properties of Low-Molecular-Weight Hydrogelators. *Langmuir* **2019**, *35*, 6506–6521.
- (8) Torres-Martinez, A.; Angulo-Pachon, C. A.; Galindo, F.; Miravet, J. F. In between Molecules and Self-Assembled Fibrillar Networks: Highly Stable Nanogel Particles from a Low Molecular Weight Hydrogelator. *Soft Matter* **2019**, *15*, 3565–3572.
- (9) Giano, M. C.; Ibrahim, Z.; Medina, S. H.; Sarhane, K. A.; Christensen, J. M.; Yamada, Y.; Brandacher, G.; Schneider, J. P. Injectable Bioadhesive Hydrogels with Innate Antibacterial Properties. *Nat. Commun.* **2014**, *5*, 1–9.
- (10) Kieffer, M.; Garcia, A. M.; Haynes, C. J. E.; Kralj, S.; Iglesias, D.; Nitschke, J. R.; Marchesan, S. Embedding and Positioning of Two Fe^{II}L₄ Cages in Supramolecular Tripeptide Gels for Selective Chemical Segregation. *Angew. Chemie - Int. Ed.* **2019**, *58*, 7982–7986.

- (11) Sajisha, V. S.; Maitra, U. Remarkable Isomer-Selective Gelation of Aromatic Solvents by a Polymorph of a Urea-Linked Bile Acid–amino Acid Conjugate. *RSC Adv.* **2014**, *4*, 43167–43171.
- (12) Marchesan, S.; Styan, K. E.; Easton, C. D.; Waddington, L.; Vargiu, A. V. Higher and Lower Supramolecular Orders for the Design of Self-Assembled Heterochiral Tripeptide Hydrogel Biomaterials. *J. Mater. Chem. B* **2015**, *3*, 8123–8132.
- (13) Vemula, P. K.; John, G. Smart Amphiphiles: Hydro/Organogelators for in Situ Reduction of Gold. *Chem. Commun.* **2006**, *21*, 2218–2220.
- (14) Beckers, S. J.; Parkinson, S.; Wheeldon, E.; Smith, D. K. In Situ Aldehyde-Modification of Self-Assembled Acyl Hydrazide Hydrogels and Dynamic Component Selection from Complex Aldehyde Mixtures. *Chem. Commun.* **2019**, *55*, 1947–1950.
- (15) Pappas, C. G.; Shafi, R.; Sasselli, I. R.; Siccardi, H.; Wang, T.; Narang, V.; Abzalimov, R.; Wijerathne, N.; Ulijn, R. V. Dynamic Peptide Libraries for the Discovery of Supramolecular Nanomaterials. *Nat. Nanotechnol.* **2016**, *11*, 960–967.
- (16) Edwards-Gayle, C. J. C.; Castelletto, V.; Hamley, I. W.; Barrett, G.; Greco, F.; Hermida-Merino, D.; Rambo, R. P.; Seitsonen, J.; Ruokolainen, J. Self-Assembly, Antimicrobial Activity, and Membrane Interactions of Arginine-Capped Peptide Bola-Amphiphiles. *ACS Appl. Bio Mater.* **2019**, *2*, 2208–2218.
- (17) Abdallah, D. J.; Sirchio, S. A.; Weiss, R. G. Hexatriacontane Organogels. The First Determination of the Conformation and Molecular Packing of a Low-Molecular-Mass Organogelator in Its Gelled State. *Langmuir* **2000**, *16*, 7558–7561.

- (18) Terech, P.; Weiss, R. G. Low Molecular Mass Gelators of Organic Liquids and the Properties of Their Gels. *Chem. Rev.* **2002**, *97*, 3133–3160.
- (19) Sangeetha, N. M.; Maitra, U. Supramolecular Gels: Functions and Uses. *Chem. Soc. Rev.* **2005**, *34*, 821–836.
- (20) Basu, K.; Mondal, B.; Das Mahapatra, A.; Nandi, N.; Basak, D.; Banerjee A. Modulation of Semiconducting Behavior and a Change in Morphology upon Gelation of a Peptide Appended Naphthalenediimide. *J. Phys. Chem. C* **2019**, *123*, 20558–20566.
- (21) Lampel, A.; Ulijn, R. V.; Tuttle, T. Guiding Principles for Peptide Nanotechnology through Directed Discovery. *Chem. Soc. Rev.* **2018**, *47*, 3737–3758.
- (22) Niu, D.; Jiang, Y.; Ji, L.; Ouyang, G.; Liu, M. Self-Assembly through Coordination and π -Stacking: Controlled Switching of Circularly Polarized Luminescence. *Angew. Chemie - Int. Ed.* **2019**, *58*, 5946–5950.
- (23) Foster, J. A.; Damodaran, K. K.; Maurin, A.; Day, G. M.; Thompson, H. P. G.; Cameron, G. J.; Bernal, J. C.; Steed, J. W. Pharmaceutical Polymorph Control in a Drug-Mimetic Supramolecular Gel. *Chem. Sci.* **2016**, *8*, 78–84.
- (24) Adler-Abramovich, L.; Gazit, E. The Physical Properties of Supramolecular Peptide Assemblies: From Building Block Association to Technological Applications. *Chem. Soc. Rev.* **2014**, *43*, 6881–6893.
- (25) Bera, S.; Mondal, S.; Xue, B.; Shimon, L. J. W.; Cao, Y.; Gazit, E. Rigid Helical-like Assemblies from a Self-Aggregating Tripeptide. *Nat. Mater.* **2019**, *18*, 503–509.

- (26) Baral, A.; Roy, S.; Dehsorkhi, A.; Hamley, I. W.; Mohapatra, S.; Ghosh, S.; Banerjee, A. Assembly of an Injectable Noncytotoxic Peptide-Based Hydrogelator for Sustained Release of Drugs. *Langmuir* **2014**, *30*, 929–936.
- (27) Sun, J. E. P.; Stewart, B.; Litan, A.; Lee, S. J.; Schneider, J. P.; Langhans, S. A.; Pochan, D. J. Sustained Release of Active Chemotherapeutics from Injectable-Solid β -Hairpin Peptide Hydrogel. *Biomater. Sci.* **2016**, *4*, 839–848.
- (28) Basu, K.; Baral, A.; Basak, S.; Dehsorkhi, A.; Nanda, J.; Bhunia, D.; Ghosh, S.; Castelletto, V.; Hamley, I. W.; Banerjee, A. Peptide Based Hydrogels for Cancer Drug Release: Modulation of Stiffness, Drug Release and Proteolytic Stability of Hydrogels by Incorporating d-Amino Acid Residue(s). *Chem. Commun.* **2016**, *52*, 5045–5048.
- (29) Mayr, J.; Saldias, C.; Diaz Diaz, D. Release of Small Bioactive Molecules from Physical Gels. *Chem. Soc. Rev.* **2018**, *47*, 1484–1515.
- (30) Qin, L.; Xie, F.; Duan, P.; Liu, M. A Peptide Dendron-Based Shrinkable Metallo-Hydrogel for Charged Species Separation and Stepwise Release of Drugs. *Chem. - A Eur. J.* **2014**, *20*, 15419–15425.
- (31) Miotto, M.; Gouveia, R. M.; Ionescu, A. M.; Figueiredo, F.; Hamley, I. W.; Connon, C. J. 4D Corneal Tissue Engineering: Achieving Time-Dependent Tissue Self-Curvature through Localized Control of Cell Actuators. *Adv. Funct. Mater.* **2019**, *29*, 1807334.
- (32) Dou, X. Q.; Feng, C. L. Amino Acids and Peptide-Based Supramolecular Hydrogels for Three-Dimensional Cell Culture. *Adv. Mater.* **2017**, *29*, 1604062.

- (33) Chakraborty, P.; Guterman, T.; Adadi, N.; Yadid, M.; Brosh, T.; Adler-Abramovich, L.; Dvir, T.; Gazit, E. A Self-Healing, All-Organic, Conducting, Composite Peptide Hydrogel as Pressure Sensor and Electrogenic Cell Soft Substrate. *ACS Nano* **2019**, *13*, 163–175.
- (34) Nandi, N.; Gayen, K.; Ghosh, S.; Bhunia, D.; Kirkham, S.; Sen, S. K.; Ghosh, S.; Hamley, I. W.; Banerjee, A. Amphiphilic Peptide-Based Supramolecular, Noncytotoxic, Stimuli-Responsive Hydrogels with Antibacterial Activity. *Biomacromolecules* **2017**, *18*, 3621–3629.
- (35) Matson, J. B.; Stupp, S. I. Self-Assembling Peptide Scaffolds for Regenerative Medicine. *Chem. Commun.* **2012**, *48*, 26–33.
- (36) Boekhoven, J.; Stupp, S. I. 25th Anniversary Article: Supramolecular Materials for Regenerative Medicine. *Adv. Mater.* **2014**, *26*, 1642–1659.
- (37) Hirst, A. R.; Escuder, B.; Miravet, J. F.; Smith, D. K. High-Tech Applications of Self-Assembling Supramolecular Nanostructured Gel-Phase Materials: From Regenerative Medicine to Electronic Devices. *Angew. Chemie - Int. Ed.* **2008**, *47*, 8002–8018.
- (38) Basak, S.; Nandi, N.; Paul, S.; Hamley, I. W.; Banerjee, A. A Tripeptide-Based Self-Shrinking Hydrogel for Waste-Water Treatment: Removal of Toxic Organic Dyes and Lead (Pb²⁺) Ions. *Chem. Commun.* **2017**, *53*, 5910–5913.
- (39) Nandi, N.; Baral, A.; Basu, K.; Roy, S.; Banerjee, A. A Dipeptide-Based Superhydrogel: Removal of Toxic Dyes and Heavy Metal Ions from Waste Water. *Pept. Sci.* **2017**, *108*, e22915. doi:10.1002/bip.22915.

- (40) Okesola, B. O.; Smith, D. K. Applying Low-Molecular Weight Supramolecular Gelators in an Environmental Setting-Self-Assembled Gels as Smart Materials for Pollutant Removal. *Chem. Soc. Rev.* **2016**, *45*, 4226–4251.
- (41) Wood, D. M.; Acton, A. L.; Rodríguez-llansola, F.; Murray, C. A.; Cardin, C. J.; Miravet, J. F.; Escuder, B.; Hamley, I. W.; Hayes, W. pH-Tunable Hydrogelators for Water Purification: Structural Optimisation and Evaluation. *Chem. Eur. J.* **2012**, *18*, 2692–2699.
- (42) Rodríguez-Llansola, F.; Escuder, B.; Miravet, J. F.; Hermida-merino, D.; Hamley, I. W.; Cardin, J.; Hayes, W. Selective and Highly Efficient Dye Scavenging by a pH-Responsive Molecular Hydrogelator. *Chem. Commun.* **2010**, *46*, 7960–7962.
- (43) Bhattacharya, S.; Krishnan-Ghosh, Y. First Report of Phase Selective Gelation of Oil from Oil/Water Mixtures. Possible Implications toward Containing Oil Spills. *Chem. Commun.* **2001**, 185–186.
- (44) Prathap, A.; Sureshan, K. M. Organogelator–Cellulose Composite for Practical and Eco-Friendly Marine Oil-Spill Recovery. *Angew. Chemie - Int. Ed.* **2017**, *56*, 9405–9409.
- (45) Basu, K.; Nandi, N.; Mondal, B.; Dehsorkhi, A.; Hamley, I. W.; Banerjee, A. Peptide-Based Ambidextrous Bifunctional Gelator: Applications in Oil Spill Recovery and Removal of Toxic Organic Dyes for Waste Water Management. *Interface Focus* **2017**, *7*, 20160128. [doi:10.1098/rsfs.2016.0128](https://doi.org/10.1098/rsfs.2016.0128).

- (46) Jadhav, S. R.; Vemula, P. K.; Kumar, R.; Raghavan, S. R.; John, G. Sugar-Derived Phase-Selective Molecular Gelators as Model Solidifiers for Oil Spills. *Angew. Chemie - Int. Ed.* **2010**, *49*, 7695–7698.
- (47) Prathap, A.; Sureshan, K. M. Sugar-Based Organogelators for Various Applications. *Langmuir* **2019**, *35*, 6005–6014.
- (48) Basak, S.; Nanda, J.; Banerjee, A. A New Aromatic Amino Acid Based Organogel for Oil Spill Recovery. *J. Mater. Chem.* **2012**, *22*, 11658–11664.
- (49) Wu, J.; Tian, Q.; Hu, H.; Xia, Q.; Zou, Y.; Li, F.; Yi, T.; Huang, C. Self-Assembly of Peptide-Based Multi-Colour Gels Triggered by up-Conversion Rare Earth Nanoparticles. *Chem. Commun.* **2009**, *27*, 4100–4102.
- (50) Palui, G.; Nanda, J.; Ray, S.; Banerjee, A. Fabrication of Luminescent CdS Nanoparticles on Short-Peptide-Based Hydrogel Nanofibers: Tuning of Optoelectronic Properties. *Chem. - A Eur. J.* **2009**, *15*, 6902–6909.
- (51) Adhikari, B.; Banerjee, A. Short-Peptide-Based Hydrogel: A Template for the in Situ Synthesis of Fluorescent Silver Nanoclusters by Using Sunlight. *Chem. - A Eur. J.* **2010**, *16*, 13698–13705.
- (52) Slavik, P.; Kurka, D. W.; Smith, D. K. Palladium-Scavenging Self-Assembled Hybrid Hydrogels-Reusable Highly-Active Green Catalysts for Suzuki-Miyaura Cross-Coupling Reactions. *Chem. Sci.* **2018**, *9*, 8673–8681.

- (53) Gayen, K.; Basu, K.; Bairagi, D.; Castelletto, V.; Hamley, I. W.; Banerjee, A. Amino-Acid-Based Metallo-Hydrogel That Acts Like an Esterase. *ACS Appl. Bio Mater.* **2018**, *1*, 1717–1724.
- (54) Zhou, G.; Liu, C.; Tang, Y.; Luo, S.; Zeng, Z.; Liu, Y.; Xu, R.; Chu, L. Sponge-like Polysiloxane-Graphene Oxide Gel as a Highly Efficient and Renewable Adsorbent for Lead and Cadmium Metals Removal from Wastewater. *Chem. Eng. J.* **2015**, *280*, 275–282.
- (55) Miao, K.; Luo, X.; Wang, W.; Guo, J.; Guo, S.; Cao, F.; Hu, Y.; Chang, P.; Feng, G. One-Step Synthesis of Cu – SBA-15 under Neutral Condition and Its Oxidation Catalytic Performance. *Micropor. Mesopor. Mater.* **2019**, *289*, 109640.
- (56) Shi, X.; Wang, C.; Ma, Y.; Liu, H.; Wu, S.; Shao, Q.; He, Z.; Guo, L. Template-Free Microwave-Assisted Synthesis of FeTi Coordination Complex Yolk-Shell Microspheres for Superior Catalytic Removal of Arsenic and Chemical Degradation of Methylene Blue from Polluted Water. *Powder Technol.* **2019**, *356*, 726–734.
- (57) Sun, L.; Shao, Q.; Zhang, Y.; Jiang, H.; Ge, S.; Lou, S.; Lin, J.; Zhang, J.; Wu, S.; Dong, M.; Guo, Z. N Self-Doped ZnO Derived from Microwave Hydrothermal Synthesized Zeolitic Imidazolate Framework-8 toward Enhanced Photocatalytic Degradation of Methylene Blue. *J. Colloid Interface Sci.* **2020**, *565*, 142-155.
- (58) WHO. Exposure to Mercury: A Major Public Health Concern. *Prev. Dis. Through Heal. Environ.* **2006**, *4*. [doi:10.1016/j.ecoenv.2011.12.007](https://doi.org/10.1016/j.ecoenv.2011.12.007).

- (59) Gong, K.; Guo, S.; Zhao, Y.; Hu, Q.; Liu, H.; Sun, D.; Li, M.; Qiu, B.; Guo, Z. Bacteria Cell Templated Porous Polyaniline Facilitated Detoxification and Recovery of Hexavalent Chromium. *J. Mater. Chem. A* **2018**, *6*, 16824–16832.
- (60) Yuan, Y.; Yu, Q.; Wen, J.; Li, C.; Guo, Z.; Wang, X.; Wang, N. Uranium Extraction Ultrafast and Highly Selective Uranium Extraction from Seawater by Hydrogel-like Spidroin-Based Protein Fiber. *Angew. Chem. Int. Ed.* **2019**, *58*, 11785–11790.
- (61) Zhao, S.; Yuan, Y.; Yu, Q.; Niu, B.; Liao, J.; Guo, Z.; Wang, N. Uranium Extraction A Dual-Surface Amidoximated Halloysite Nanotube for High-Efficiency Economical Uranium Extraction from Seawater. *Angew. Chem. Int. Ed.* **2019**, *58*, 14979–14985.
- (62) Qian, Y.; Yuan, Y.; Wang, H.; Liu, H.; Zhang, J.; Shi, S.; Guo, Z.; Wang, N. Salicylaldoxime / Polydopamine Graphene Oxide. *J. Mater. Chem. A* **2018**, *6*, 24676–24685.
- (63) Wang, Y.; Zhou, P.; Luo, S.; Liao, X.; Wang, B.; Shao, Q.; Guo, X.; Guo, Z. Controllable Synthesis of Monolayer Poly(Acrylic Acid) on the Channel Surface of Mesoporous Alumina for Pb(II) Adsorption. *Langmuir* **2018**, *34*, 7859–7868.
- (64) Sankhla, M. S.; Kumari, M.; Nandan, M.; Kumar, R.; Agrawal, P. Heavy Metals Contamination in Water and Their Hazardous Effect on Human Health-A Review. *Int. J. Curr. Microbiol. Appl. Sci.* **2016**, *5*, 759–766.
- (65) Achary, M. S.; Satpathy, K. K.; Panigrahi, S.; Mohanty, A. K.; Padhi, R. K.; Biswas, S.; Prabhu, R. K.; Vijayalakshmi, S.; Panigrahy, R. C. Concentration of Heavy Metals in the Food

Chain Components of the Nearshore Coastal Waters of Kalpakkam, Southeast Coast of India.

Food Control **2017**, 72, 232–243.

(66) Merrill J.C., Morton J.J.P., Soileau S.D., Metals. In: Hayes A.W, editor. Principles and Methods of Toxicology. 5th ed. CRC Press; **2007**.

(67) Jarup, L. Hazards of Heavy Metal Contamination. *Br. Med. Bull.* **2003**, 68, 167–182.

(68) Van Der Bruggen, B.; Vandecasteele, C.; Van Gestel, T.; Doyen, W.; Leysen, R. A Review of Pressure-Driven Membrane Processes in Wastewater Treatment and Drinking Water Production. *Environ. Prog.* **2003**, 22, 46–56.

(69) Chowdhury, A.; Khan, A. A.; Kumari, S.; Hussain, S. Superadsorbent Ni-Co-S/SDS Nanocomposites for Ultrahigh Removal of Cationic, Anionic Organic Dyes and Toxic Metal Ions: Kinetics, Isotherm and Adsorption Mechanism. *ACS Sustain. Chem. Eng.* **2019**, 7, 4165–4176.

(70) Maiti, D.; Mukhopadhyay, S.; Devi, P. S. Evaluation of Mechanism on Selective, Rapid, and Superior Adsorption of Congo Red by Reusable Mesoporous α -Fe₂O₃ Nanorods. *ACS Sustain. Chem. Eng.* **2017**, 5, 11255–11267.

(71) Ramalingam, B.; Parandhaman, T.; Choudhary, P.; Das, S. K. Biomaterial Functionalized Graphene-Magnetite Nanocomposite: A Novel Approach for Simultaneous Removal of Anionic Dyes and Heavy-Metal Ions. *ACS Sustain. Chem. Eng.* **2018**, 6, 6328–6341.

(72) Ray, S.; Das, A. K.; Banerjee, A. pH-Responsive, Bolaamphiphile-Based Smart Metallo-Hydrogels as Potential Dye-Adsorbing Agents, Water Purifier, and Vitamin B₁₂ Carrier. *Chem. Mater***2007**, *19*, 1633–1639.

(73) Minju, N.; Jobin, V.; Savithri, S.; Ananthakumar, S. Double-Silicate Derived Hybrid Foams for High-Capacity Adsorption of Textile Dye Effluent: Statistical Optimization and Adsorption Studies. *Langmuir***2019**, *35*, 9382–9395.

(74) Zhang, X.; Pan, Y.; Zhao, J.; Hao, X.; Wang, Y.; Schubert, D. W.; Liu, C.; Shen, C.; Liu, X. Facile Construction of Copper Mesh Surface from Superhydrophilic to Superhydrophobic for Various Oil-Water Separations. *Eng. Sci.***2019**, *7*, 65–71.

(75) Cai, J.; Tian, J.; Gu, H.; Guo, Z. Amino Carbon Nanotube Modified Reduced Graphene Oxide Aerogel for Oil/Water Separation. *ES Mater. Manuf.***2019**, *6*, 68–74.

(76) Kayan, A. Inorganic-organic hybrid materials and their adsorbent properties. *Advanced Composites and Hybrid Materials*. Doi:10.1007/s42114-018-0073-y.

(77) Zhang, J.; Li, P.; Zhang, Z.; Wang, X.; Tang, J.; Liu, H.; Shao, Q.; Ding, T.; Umar, A.; Guo, Z. Solvent-Free Graphene Liquids: Promising Candidates for Lubricants without the Base Oil. *J. Colloid Interface Sci.***2019**, *542*, 159–167.

(78) Hu, W.; Huang, J.; Zhang, X.; Zhao, S.; Pei, L.; Zhang, C.; Liu, Y.; Wang, Z. A Mechanically Robust and Reversibly Wetttable Benzoxazine/ Epoxy/ Mesoporous TiO₂ Coating for Oil/Water Separation. *Appl. Surf. Sci.***2020**, *507*, 145168.

- (79) Wen, N.; Jiang, B.; Wang, X.; Shang, Z.; Jiang, D.; Zhang, L.; Sun, C.; Wu, Z.; Yan, H.; Liu, C.; Guo, Z. Overview of Polyvinyl Alcohol Nanocomposite Hydrogels for Electro-Skin, Actuator, Supercapacitor and Fuel cell. *Chem. Rec.***2020**, *20*, 773–792.
- (80) Wei, H. G.; Wang, H.; Li, A.; Cui, D. P.; Zhao, Z. N.; Chu, L. Q.; Wei, X.; Wang, L.; Pan, D.; Fan, J. C.; Li, Y. C.; Zhang, J. X.; Liu, C. T.; Wei, S. Y.; Guo, Z. H. Multifunctions of Polymer Nanocomposites: Environmental Remediation, Electromagnetic Interference Shielding, And Sensing Applications. *ChemNanoMat***2020**, *6*, 1–12.
- (81) Gu, H.; Zhang, H.; Gao, C.; Liang, C.; Gu, J.; Guo, Z. New Functions of Polyaniline. *ES Mater. Manuf.***2018**, *1*, 3–12.
- (82) Xie, P.; Li, Y.; Hou, Q.; Sui, K.; Liu, C.; Fu, X.; Zhang, J.; Murugadoss, V.; Fan, J.; Wang, Y.; Fan, R.; Guo, Z. Tunneling-Induced Negative Permittivity in Ni/MnO Nanocomposites by a Bio-Gel Derived strategy. *J. Mater. Chem. C***2020**, *8*, 3029–3039.
- (83) Zhang, L.; Jiang, D.; Dong, T.; Das, R.; Pan, D.; Sun, C.; Wu, Z.; Zhang, Q.; Liu, C.; Guo, Z. Overview of Ionogels in Flexible Electronics. *Chem. Rec.***2020**, *20*, 1–21.
- (84) Zhou, N.; Wang, T.; Chen, S.; Hu, Q.; Cheng, X.; Sun, D.; Vupputuri, S.; Qiu, B.; Liu, H.; Guo, Z. Conductive Polyaniline Hydrogel Enhanced Methane Production from Anaerobic Wastewater Treatment. *J. Colloid Interface Sci.***2021**, *581*, 314–322.
- (85) Zhang, Y.; Xie, S.; Zhang, D.; Ren, B.; Liu, Y.; Tang, L.; Chen, Q.; Yang, J.; Wu, J.; Tang, J.; Zheng, J. Thermo-Responsive and Shape-Adaptive Hydrogel Actuators from Fundamentals to Applications. *Eng. Sci.***2019**, *6*, 1–11.

- (86) Li, S.; Jasim, A.; Zhao, W.; Fu, L.; Ullah, M. W.; Shi, Z.; Yang, G. Fabrication of pH-Electroactive Bacterial Cellulose / Polyaniline Hydrogel for the Development of a Controlled Drug Release System. *ES Mater. Manuf.***2018**, *1*, 41–49.
- (87) Ul-islam, M.; Ali, J.; Khan, W.; Haider, A.; Shah, N.; Ahmad, W.; Ullah, M. W.; Yang, G. Fast 4-Nitrophenol Reduction Using Gelatin Hydrogel Containing Silver Nanoparticles. *Eng. Sci.***2019**, *8*, 19–24.
- (88) Huang, H.; Han, L.; Wang, Y.; Yang, Z.; Zhu, F.; Xu, M. Tunable Thermal-Response Shape Memory Bio-Polymer Hydrogels as Body Motion Sensors. *Eng. Sci.* **2020**, *9*, 60–67.
- (89) Sun, L.; Shi, Z.; Wang, H.; Zhang, K.; Dastan, D.; Sund, K.; Fand, R. Ultrahigh Discharge Efficiency and Improved Energy Density in Rationally Designed Bilayer Polyetherimide–BaTiO₃/P(VDF-HFP) Composites. *J. Mater. Chem. A***2020**, *8*, 5750–5757.
- (90) Sun, K.; Wang, L.; Wang, Z.; Wu, X.; Fan, G.; Wang, Z.; Cheng, C.; Fan, R.; Dongef, M.; Guo, Z. Flexible Silver Nanowire/Carbon Fiber Felt Metacomposites with Weakly Negative Permittivity Behavior. *Phys. Chem. Chem. Phys.***2020**, *22*, 5114–5122.
- (91) Wang, Z.; Sun, K.; Xie, P.; Liu, Y.; Gu, Q.; Fan, R. Permittivity Transition from Positive to Negative in Acrylic Polyurethane-Aluminum Composites. *Compos. Sci. Technol.***2020**, *188*, 107969.
- (92) Sun, K.; Wang, Z.; Xin, J.; Wang, Z.; Xie, P.; Fan, G.; Murugadoss, V.; Fan, R.; Fan, J.; Guo, Z. Hydrosoluble Graphene/Polyvinyl Alcohol Membranous Composites with Negative Permittivity Behavior. *Macromol. Mater. Eng.***2020**, *305*, 1900709.

- (93) Hu, J.; Lin, J.; Zhang, Y.; Lin, Z.; Qiao, Z.; Liu, Z.; Yang, W.; Liu, X.; Dong, M.; Guo, Z. A New Anti-Biofilm Strategy of Enabling Arbitrary Surfaces of Materials and Devices with Robust Bacterial Anti-Adhesion via a Spraying Modified Microsphere Method. *J. Mater. Chem. A***2019**, *7*, 26039–26052.
- (94) Zheng, C.; Zhang, P.; Cheng, J.; Guo, Z.; Liu, H. Durably Antibacterial and Bacterially Antiadhesive Cotton Fabrics Coated by Cationic Fluorinated Polymers. *ACS Appl. Mater. Interfaces***2018**, *10*, 6124–6136.
- (95) Cheng, N.; Hu, Q.; Guo, Y.; Wang, Y.; Yu, L. Efficient and Selective Removal of Dyes Using Imidazolium-Based Supramolecular Gels. *ACS Appl. Mater. Interfaces***2015**, *7*, 10258–10265.
- (96) Karan, C. K.; Bhattacharjee, M. Self-Healing and Moldable Metallogels as the Recyclable Materials for Selective Dye Adsorption and Separation. *ACS Appl. Mater. Interfaces***2016**, *8*, 5526–5535.
- (97) Zhang, X.; Liu, D.; Yang, L.; Zhou, L.; You, T. Self-assembled Three-Dimensional Graphene-Based Materials for Dye Adsorption and Catalysis. *J. Mater. Chem. A***2015**, *3*, 10031–10037.
- (98) Li, D.; Li, Q.; Bai, N.; Dong, H.; Mao, D. One-Step Synthesis of Cationic Hydrogel for Efficient Dye Adsorption and Its Second Use for Emulsified Oil Separation. *ACS Sustainable Chem. Eng.***2017**, *5*, 5598–5607.

- (99) Zhang, H.; Lyu, S.; Zhou, X.; Gu, H.; Ma, C.; Wang, C. Super Light 3D Hierarchical Nanocellulose Aerogel Foam with Superior Oil Adsorption. *J. Colloid Interface Sci.***2019**, *536*, 245-251.
- (100) Gu, H.; Zhou, X.; Lyu, S.; Pan, D.; Dong, M.; Wu, S. Magnetic Nanocellulose-Magnetite Aerogel for Easy Oil Adsorption. *J. Colloid Interface Sci.***2020**, *560*, 849–856.
- (101) Sun, S.; Zhu, L.; Liu, X.; Wu, L.; Dai, K.; Liu, C.; Shen, C.; Guo, X.; Zheng, G.; Guo, Z. Superhydrophobic Shish-Kebab Membrane with Self-Cleaning and Oil/Water Separation Properties. *ACS Sustainable Chem. Eng.***2018**, *6*, 9866–9875.
- (102) Zhang, J.; Wang, Z.; Shen, C.; Guo, Z. Superhydrophobic/Superoleophilic Polycarbonate/Carbon Nanotubes Porous Monolith for Selective Oil Adsorption from Water. *ACS Sustainable Chem. Eng.***2018**, *6*, 13747–13755.

Graphical abstract:

